Controlling HD^+ and H_2^+ Dissociation with the Carrier-Envelope Phase Difference of an Intense Ultrashort Laser Pulse

Vladimir Roudnev, B. D. Esry, and I. Ben-Itzhak

J. R. Macdonald Laboratory, Kansas State University, Manhattan, Kansas 66506, USA

(Received 19 May 2004; published 13 October 2004)

Carrier-envelope phase difference effects in the dissociation of the HD^+ molecular ion in the field of an intense, linearly polarized, ultrashort laser pulse are studied in the framework of the time-dependent Schrödinger equation. We consider a reduced-dimensionality model in which the nuclei are free to vibrate along the field polarization and the electrons move in two dimensions. The laser has a central wavelength of 790 nm and a pulse length of 10 fs with intensities in the range 6×10^{14} to 9×10^{14} W/cm^2. We find that the angular distribution of dissociation to $p + \mathrm{D}$ and $\mathrm{H} + d$ can be controlled by varying the phase difference, generating differences between the dissociation channels of more than a factor of 2. Moreover, the asymmetry is nearly as large for H_2^+ dissociation.

DOI: 10.1103/PhysRevLett.93.163601 PACS numbers: 42.50.Hz, 33.80.Eh, 33.80.Wz

Diatomic molecules and molecular ions in intense laser fields continue to attract the attention of the atomic and molecular physics community despite several years of study. The nonperturbative nature of the laser field coupled with the interplay of the electronic and nuclear degrees of freedom make for very rich physics. It is, of course, precisely these properties that also make these systems such a challenge to treat theoretically.

The hydrogen molecular ion is of special interest since it is the simplest molecule, consisting of three particles only. Even so, it exhibits many interesting phenomena including bond hardening (or vibrational trapping) and bond softening [1–3], high harmonic generation [4], above threshold dissociation [5], and enhanced ionization [6,7].

Other studies [8] have shown that the relative phase between two laser pulses with different central frequencies could be used to control the dissociation of HD^+. The main finding was that the angular distributions of H and D depended differently on the relative phase of the two laser pulses—where H had a maximum, D had a minimum and vice versa.

More recently, it has become possible to measure [9] and control [10] the carrier-envelope phase difference (CEPD) of a single ultrashort laser pulse, i.e., the relative phase between the laser pulse envelope and the carrier frequency. These experiments took advantage of the CEPD dependence of the photoelectron angular distributions. A recent theoretical treatment [11] predicts that the angular asymmetry is present only for pulses less than 15 cycles in duration.

The central question we consider in this work is whether it is possible to observe CEPD effects in the dissociation of HD^+ in a short (≈ 10 fs) linearly polarized laser pulse. There are, of course, two different dissociation channels:

$$\mathrm{HD}^+ + n\gamma \rightarrow \begin{cases} \mathrm{H} + d \\ p + \mathrm{D} \end{cases}.$$

Is dissociation to one of the channels more probable than to the other? If so, under what conditions? Stated another way, we are asking to what extent can this reaction be controlled—a question normally associated with coherent control.

Our answer to these questions will come from solving the time-dependent Schrödinger equation. A full solution to this problem would require the propagation of a six-dimensional wave function. Unfortunately, this task is beyond our current capability. We must, therefore, use physical reasoning and intuition to reduce the dimensionality to something manageable that also retains the essential physics of the problem.

Various reduced-dimensionality models have been proposed and studied. Some have assumed the Born-Oppenheimer approximation and included two electronic degrees of freedom [12,13]; others have carried out non-Born-Oppenheimer calculations, including nuclear vibration along with either one [14–16] or two [17–19] electronic degrees of freedom. All of these models have shared the assumption that the molecule does not have time to rotate significantly during the laser pulse. Combined with the fact that the molecules dissociate primarily along the laser polarization, this assumption was used to fix the nuclei along the polarization direction. Experimentally, this assumption can actually be satisfied in two ways: by aligning the molecules or by selecting only those fragments that came from aligned molecules using, for instance, three-dimensional momentum imaging.

The three-dimensional model (one nuclear plus two electronic degrees of freedom) is currently the state of the art for H_2^+ in a short, intense laser pulse and is the one we choose for the present studies. First, we expect non-Born-Oppenheimer effects to be significant since the laser field couples primarily to the electron (even for HD^+). Dissociation must thus proceed via energy exchange between the electron and nuclei. Second, among the non-Born-Oppenheimer approaches, it is the lowest di-

mensional model that retains the physical Coulomb potential. That is, no softening of the Coulomb potential is required, unlike the two-dimensional non-Born-Oppenheimer model. This point is critical since it was recently shown [20] that the dissociation and ionization probabilities depend very sensitively on how the Coulomb singularities are softened. Moreover, the three-dimensional model has, in principle, the correct energy spectrum for both the electrons and the nuclei, which is not true in the two-dimensional model.

We solve the time-dependent Schrödinger equation (atomic units will be used unless otherwise noted)

$$i\frac{\partial}{\partial t}\psi(\mathbf{R}, \mathbf{r}, t) = [H_0 + V(t)]\psi(\mathbf{R}, \mathbf{r}, t), \tag{1}$$

where H_0 is the field-free HD^+ Hamiltonian. The potential $V(t)$ includes the interaction of the particles with the laser pulse, $\mathbf{R}$ is the internuclear vector, and the electron coordinate $\mathbf{r}$ is measured from the center of mass of the nuclei. It is chosen so that the proton lies along the positive z axis. Since we will only consider initial σ electronic states, the azimuthal electron coordinate can be eliminated by symmetry. The six-dimensional space is then reduced to three [17–19]: (R, ρ, z), where R is the internuclear distance and (ρ, z) are the cylindrical coordinates of the electron.

The field-free Hamiltonian in the three-dimensional model is

$$H_0 = -\frac{1}{2\mu_{pd}}\frac{\partial^2}{\partial R^2} - \frac{1}{2\mu_e}\left(\frac{\partial^2}{\partial \rho^2} + \frac{1}{\rho}\frac{\partial}{\partial \rho} + \frac{\partial^2}{\partial z^2}\right) - \frac{1}{\sqrt{(z - z_p)^2 + \rho^2}} - \frac{1}{\sqrt{(z + z_d)^2 + \rho^2}} + \frac{1}{R}, \tag{2}$$

where $z_p = \frac{m_d}{m_p + m_d}R$ and $z_d = \frac{m_p}{m_p + m_d}R$ are the positions of the proton and deuteron, respectively. In this expression, μ_{pd} and μ_e are the reduced masses,

$$\frac{1}{\mu_{pd}} = \frac{1}{m_p} + \frac{1}{m_d} \quad \text{and} \quad \frac{1}{\mu_e} = 1 + \frac{1}{m_p + m_d}. \tag{3}$$

The interaction with the laser is treated in the dipole approximation (length gauge),

$$V(t) = E(t)\left[\frac{m_d - m_p}{m_p + m_d}R - \frac{m_p + m_d + 2}{m_p + m_d + 1}z\right], \tag{4}$$

in which the laser pulse takes the form

$$E(t) = E_0 e^{-(t/\tau)^2}\cos(\omega t + \phi). \tag{5}$$

In this expression, τ is the pulse duration, ω is the central laser frequency, ϕ is the CEPD with respect to the pulse peak position, and E_0 is the peak electric field amplitude in atomic units [21].

In order to solve Eq. (1) numerically, we construct discrete analogs of the operators H_0 and $V(t)$ using the finite difference method described in the appendix of Ref. [22] (and references therein). This version has the advantage that essentially arbitrary volume elements can be incorporated, yet the kinetic energy matrix remains symmetric and the underlying wave function remains analytic. In addition, this formulation of finite differences allows any distribution of grid points, not just uniform grids.

Solutions of the time-dependent Schrödinger equation can be found using the short-time propagator

$$\psi(t + \delta) \approx e^{-i\{H_0 + V[t + (\delta/2)]\}\delta}\psi(t). \tag{6}$$

To evaluate the exponential, we split the kinetic from the potential energy operators, taking into account that the kinetic energy operators T_R, T_ρ, and T_z commute. The potential operator includes all the potential energy of the system plus a purely imaginary term W to produce an absorbing boundary.

The calculations can be sped up considerably by arranging the evolution operator to take advantage of the disparity in the time scales of the nuclear and electronic motion. We can estimate this ratio to be $N = \sqrt{\mu_{pd}/\mu_e}$, assuming that the energy pumped into the nuclear motion by the laser is the same as for the electron. The resulting time evolution operator is

$$U(t + \delta, t) = U_{T_R}\left(\frac{\delta}{2}\right)\left[\prod_i^N U_e\left(\frac{\delta}{N}; t_i\right)\right]U_{T_R}\left(\frac{\delta}{2}\right). \tag{7}$$

where the electronic evolution operator is

$$U_e\left(\frac{\delta}{N}; t_i\right) = U_V\left(\frac{\delta}{2N}; t_i\right)U_{T_\rho}\left(\frac{\delta}{N}\right)U_{T_z}\left(\frac{\delta}{N}\right)U_V\left(\frac{\delta}{2N}; t_i\right)$$

with $V = V_0 + V(t + \frac{\delta}{2})$ (V_0 represents the Coulomb interactions). Each of the U operators are evaluated using the Crank-Nicolson method [23]. The electronic coordinates thus get updated N times more often than the nuclear coordinates. The rough estimate above gives $N \approx 35$. Testing, however, shows that $N = 11$ is required to obtain accurate results.

For all of the calculations reported here, the initial state was the ground state of the molecular ion, i.e., the ground vibrational state with σ electronic symmetry. This state was found by direct solution of the time-independent Schrödinger equation with the Hamiltonian given in Eq. (2). The same finite difference grid was used, and the time-independent equation was solved by propagation in imaginary time using the evolution operator from Eq. (7). The resulting ground state energy is -0.5952 a.u., compared to the accurate value -0.5980 a.u. [24].

The calculations were performed for a 790 nm, 10 fs FWHM laser pulse [$\omega = 0.058$ a.u. and $\tau = 247$ a.u. in Eq. (5)] which includes about four laser cycles. We have found that to keep the calculated dissociation probabilities accurate to 1.0%, the initial time must be chosen to be -450 a.u. The time step δ, which is associated with the nuclear motion, was set to 0.5 a.u.

The grid covers the ranges $R = 0$ to 20 a.u., $\rho = 0$ to 15 a.u., and $z = -50$ to 50 a.u. with, typically, 350, 30, and 240 points, respectively. The grid points followed a parabolic distribution to make them denser near each coordinate origin. The overall size of the grid was chosen to minimize the computation time while retaining the dissociation physics. In particular, we discarded, via the absorbing boundaries, the wave packets representing ionization, but kept the z boundary large enough to contain any electron wave packets that returned to the molecule. The leading edge of the dissociating wave packets reach the absorbing boundary at about $t = 900$ a.u., and the trailing edge leaves the grid by about $t = 2000$ a.u. The propagation for each set of laser parameters typically takes about two days on a 2 GHz Pentium 4.

Convergence testing with respect to the number of spatial grid points (varied from about 60% to at least 120% of the production grid in each coordinate) and the grid distribution leads us to deduce an accuracy of 3–5% in the dissociation probabilities, with the larger probabilities more accurately reproduced. The dissociation probabilities are most likely underestimated due mainly to small inaccuracies in representing the asymptotic atomic states on the grid.

Given that we have the time-dependent wave function on the grid, the main question is how to analyze it; specifically, how to distinguish between different reaction channels. For simplicity, we define the channels by their position in configuration space (see Fig. 1). The integral of the probability density over these regions is then the probability for the associated physical process to occur [6]. For example, the probability of dissociation into $p + \mathrm{D}$ is given by $P_D = \int_{\Omega_D} d\Omega |\psi(t \to \infty)|^2$. The probability for dissociation into $\mathrm{H} + d$, P_H, can similarly be obtained.

Our analysis assumes that highly excited states do not contribute significantly to the final state of the system. That is, the regions Ω are only large enough to contain the low-lying, well localized states. This assumption is satisfied at least visually based upon inspections of the probability density from typical calculations. Another assumption is that the ionized part of the wave function is negligibly small in each region Ω compared with the contributions coming from dissociation or excitation channels. This assumption follows from the fact that ionization produces relatively fast electrons that follow different trajectories than the dissociating fragments. Again, inspection of the probability density for typical parameters confirms this assumption.

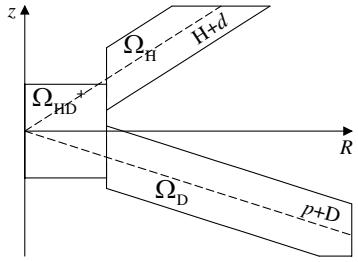

FIG. 1. Schematic of the domains in configuration space defining different final states. The difference between Ω_H and Ω_D is due to mass [see Eq. (2)].

The present analysis has the virtue of simplicity, but it is not entirely satisfactory. Only total probabilities are easily obtained, for instance, since any more detailed information would require significantly more numerical analysis. The various final configurations are only approximately separated and any errors in this separation are difficult to quantify. Empirically and intuitively we expect that the present analysis is, however, sufficiently accurate to answer the questions of interest here.

If there is complete control over the system—both CEPD and molecule orientation—then our calculations show a clear difference between the two dissociation outcomes. Further, since the laser pulse is short, we can expect substantial phase dependence of the result. Figure 2 shows the dissociation probabilities as a function of the CEPD for different laser intensities. The strong phase dependence is evident. Note that the figure shows the CEPD dependence with the proton up, i.e., at zero degrees relative to the polarization vector, and the deuteron down (180°). The same figure, however, also describes the opposite situation—deuteron at 180° and proton at 0°—if ϕ is shifted by π.

Figure 2 also shows that either of the dissociation channels can be made dominant by a careful choice of the CEPD at any intensity within the range. In fact, the ratio of the probabilities can be a factor of 2 or more over most of the intensity range shown. Such selectivity is a fundamental ingredient in coherent control schemes. Moreover, such asymmetries in atomic ionization have been used to detect the CEPD [9].

Although we have focused on HD^+ because the dissociation channels can be easily separated experimentally, it is natural to ask whether the effect is also seen in H_2^+. Figure 3 shows the dissociation probabilities of H_2^+ for an

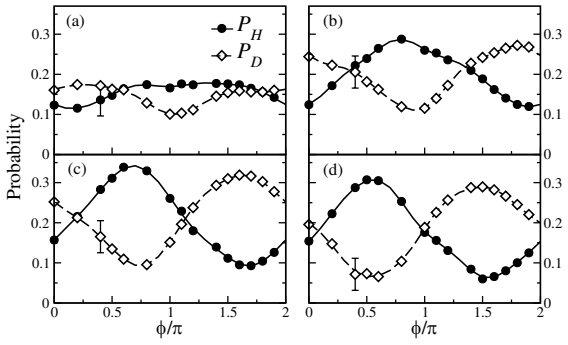

FIG. 2. Phase dependence of the HD^+ dissociation probabilities to $\mathrm{H} + d$ (solid lines) and to $p + \mathrm{D}$ (dashed lines) for different intensities: (a) $I = 6.0$, (b) $I = 7.0$, (c) $I = 8.0$, and (d) $I = 9.0$ in units of 10^{14} W/cm^2. The error bars indicate our estimated numerical error and are the same for each point in each plot.

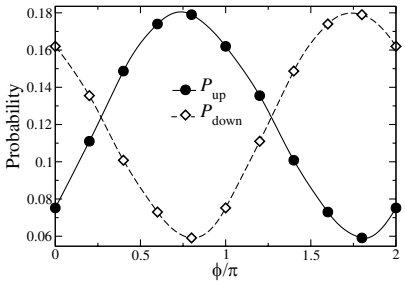

FIG. 3. Phase dependence of the H_2^+ dissociation probabilities to H at 0° (solid lines) and to H at 180° (dashed lines) for $I = 9 \times 10^{14}$ W/cm^2.

intensity of 9×10^{14} W/cm^2. The calculation was performed exactly as described for HD^+, but the probabilities now refer to H measured at 0° (P_{up}, to be compared with P_H for HD^+) and at 180° (P_{down}, P_D for HD^+).

The maximum dissociation probability in Fig. 3 is smaller than for HD^+ at the same intensity, Fig. 2(d). Otherwise, H_2^+ displays similar behavior—including up to a factor of 2 difference between P_{up} and P_{down}—except that the phase at which $P_{up} = P_{down}$ ($P_H = P_D$) is shifted by about 0.2π radians (this shift depends on intensity). We conclude that observing CEPD effects in the dissociation probabilities does not depend on the nuclear masses, but the magnitude does.

When the CEPD is controlled but the initial molecule orientation is not, then the dissociation probabilities from Fig. 2 must be averaged—that is, the proton up and down orientations averaged together. This amounts to averaging the curves in Fig. 2 at two phases of the laser: ϕ and $\phi + \pi$. The difference between the orientation-averaged dissociation probabilities does not exceed 3%, which is comparable to the accuracy of the present calculations. Thus, no substantial dissociation asymmetry is predicted with aligned—but not oriented—HD^+ in the field of a phase-controlled laser. It should be mentioned, however, that this result assumes that only the total number of dissociating H and D atoms is measured. If the angular distribution is also measured, then Fig. 2 is recovered and strong asymmetries can be seen.

Finally, if the CEPD is not controlled and the molecule not oriented, then the phase-averaged dissociation probabilities are within 1% of each other and the difference does not exceed our numerical error. In this case, however, measuring the angular distribution does not restore the asymmetry between $H + d$ and $p + D$ since the results in Fig. 2 averaged over any 2π range of the phase (mod 2π) will give the same answer. For the same reason, orienting the molecules without controlling the CEPD will show no asymmetry.

In principle, the probabilities must also be averaged over the intensity distribution in the laser focus to determine whether the CEPD effects will be observable. From Figs. 2(c) and 2(d), though, we can see that the phase dependence at 8×10^{14} W/cm^2 and 9×10^{14} W/cm^2 are nearly the same. Thus, for peak intensities in this range, the CEPD effects should survive.

We have predicted strong CEPD effects in the dissociation of HD^+ and H_2^+ in experiments that can be done with existing technology. The calculations used a three-dimensional model free from the uncertainties of softening the Coulomb potential. We conclude that if the CEPD is controlled, then the angular distribution of the dissociation products will show a strong asymmetry between 0° and 180°. Such an asymmetry can, in turn, be used to control the dissociation pathway.

We thank C. L. Cocke for useful comments on the manuscript. Support provided by the Chemical Sciences, Geosciences, and Biosciences Division, Office of Basic Energy Sciences, Office of Science, U.S. Department of Energy.

[1] A. Giusti-Suzor and F. H. Mies, Phys. Rev. Lett. **68**, 3869 (1992).
[2] E. E. Aubanel, J. M. Gauthier, and A. D. Bandrauk, Phys. Rev. A **48**, 2145 (1993).
[3] G. Yao and S. I. Chu, Phys. Rev. A **48**, 485 (1993).
[4] T. Zuo, S. Chelkowski, and A. D. Bandrauk, Phys. Rev. A **48**, 3837 (1993).
[5] A. Datta, S. Saha, and S. S. Bhattacharyya, J. Phys. B **30**, 5737 (1997).
[6] S. Chelkowski *et al.*, Phys. Rev. A **52**, 2977 (1995).
[7] L. B. Madsen and M. Plummer, J. Phys. B **31**, 87 (1998).
[8] E. Charron, A. Giusti-Suzor, and F. H. Mies, J. Chem. Phys. **103**, 7359 (1995).
[9] G. G. Paulus *et al.*, Nature (London) **414**, 182 (2001).
[10] A. Baltuska *et al.*, Nature (London) **421**, 611 (2003).
[11] S. Chelkowski and A. D. Bandrauk, Phys. Rev. A **65**, 061802 (2002).
[12] H. Yu and A. Bandrauk, J. Chem. Phys. **102**, 1257 (1995).
[13] L. Y. Peng *et al.*, J. Phys. B **36**, L295 (2003).
[14] K. C. Kulander, F. H. Mies, and K. J. Schafer, Phys. Rev. A **53**, 2562 (1996).
[15] A. D. Bandrauk, S. Chelkowski, and I. Kawata, Phys. Rev. A **67**, 13407 (2003).
[16] B. Feuerstein and U. Thumm, Phys. Rev. A **67**, 043405 (2003); **67**, 063408 (2003).
[17] D. Dundas *et al.*, Eur. Phys. J. D **26**, 51 (2003).
[18] I. Kawata, H. Kono, and Y. Fujimura, J. Chem. Phys. **110**, 11152 (1999).
[19] S. Chelkowski *et al.*, Phys. Rev. A **54**, 3235 (1996).
[20] G. L. Ver Steeg, K. Bartschat, and I. Bray, J. Phys. B **36**, 3325 (2003).
[21] We convert between intensity I in W/cm^2 and atomic units for the electric field using $E_0 = 5.33799 \times 10^{-9}\sqrt{I}$.
[22] M. W. J. Bromley and B. D. Esry, Phys. Rev. A **69**, 053620 (2004).
[23] W. H. Press, S. A. Teukolsky, W. T. Vetterling, and B. P. Flannery, *Numerical Recipes* (Cambridge, Cambridge, 1992), 2nd ed., p. 640.
[24] B. D. Esry and H. R. Sadeghpour, Phys. Rev. A **60**, 3604 (1999).